Acta Crystallographica Section D
Biological Crystallography
ISSN 0907-4449

Structure of glutaredoxin Grx1p C30S mutant from yeast

Kjell O. Håkansson* and Jakob R. Winther

Department of Molecular Biology, August Krogh Building, University of Copenhagen, Universitetsparken 13, DK-2100 Copenhagen Ø, Denmark

Correspondence e-mail: kohakansson@aki.ku.dk

Received 23 October 2006
Accepted 29 November 2006

PDB References: Grx1p C30S mutant, 2jac, r2jacsf; rxYFP-Grx1p C30S fusion protein, 2jad, r2jadsf.

Glutathionylated glutaredoxin Grx1p C30S mutant from yeast has been crystallized in space group $C222_1$ and a fusion protein between redox-sensitive yellow fluorescent protein (rxYFP) and Grx1p C30S has been crystallized in space group $P6_4$. The structure of the latter was solved by molecular replacement using the known rxYFP structure as a search model. The structure of the Grx1p moiety was built and the structure was refined against 2.7 Å synchrotron data to an $R_{\rm free}$ of 25.7%. There are no specific contacts between the two domains, indicating that the observed enhanced exchange of reduction equivalents between them arises from diffusion or from an enhanced collision rate in solution. The Grx1p structure thus obtained was subsequently used to solve the structure of the orthorhombic crystal, which could be refined against 2.0 Å data to an $R_{\rm free}$ of 24.3%. The structure of the glutathione-bound protein and the glutaredoxin domain in the fusion protein are similar. The covalent disulfide bond between the glutathione and protein is broken upon exposure to synchrotron radiation. The structure and the glutathione-binding mode are described and compared with existing crystallographic and nuclear magnetic resonance (NMR) structures of related glutaredoxins. Conserved residues are clustered on one side of the active site.

1. Introduction

Glutaredoxins act as intracellular antioxidants that catalyze the reduction of protein disulfide bonds using glutathione (γ-Glu-Cys-Gly) as the reducing agent (for a review, see Fernandes & Holmgren, 2004). They are relatively small proteins that are present in a wide variety of prokaryotic and eukaryotic organisms and in a few viruses. Most species have several glutaredoxin isoforms. The monomeric proteins, typically of 10 kDa, are structurally and functionally related to the thioredoxins, although the reduced form of the latter is regenerated through the action of thioredoxin reductase rather than by glutathione. Together, they are also essential for the production of deoxyribonucleotides by supplying ribonucleotide reductase with H atoms. In both glutaredoxin and thioredoxin, the reducing equivalents are ultimately derived from NADPH. Central to the mechanism of glutaredoxins is the active-site CP*X*C motif, where the first cysteine may be glutathionylated as part of the redox process or may form a disulfide bridge with the second cysteine. These two residues are found in the N-terminal part of an α-helix in

glutaredoxin and related proteins. A second category, the monothiol glutaredoxins, contain only the most N-proximal cysteine residue in the active site.

Grx1p is one of five characterized isoforms found in yeast. Two of these are of the dithiol variety (Grx1p and Grx2p), while the remaining three are monothiol forms (Grx3p, Grx4p and Grx5p). Grx1p has no close relative in the PDB (Berman *et al.*, 2000). The most similar sequences found in crystal structures are those of *Haemophilus influenza* Prx5 (Kim *et al.*, 2003; 22% sequence identity), a natural hybrid consisting of a peroxiredoxin domain and a glutaredoxin domain, and the recently deposited structure of human glutaredoxin 2 (28% identity; PDB code 2fls). The small size of the glutaredoxins makes them suitable for NMR studies and the structures of *Escherichia coli* glutaredoxins 1 and 3 have been investigated in various oxidation states (Nordstrand *et al.*, 1999; Sodano *et al.*, 1991; Xia *et al.*, 1992), as has the glutaredoxin C1 from *Populus tremula* × *tremuloides* (PDB codes 1z7r and 1z7p). Recently, crystallization of glutaredoxin 2 from yeast (Discola *et al.*, 2005) and a glutaredoxin from ectromelia virus (Bacik *et al.*, 2005) have been reported, but no structures have yet been published.

The enzymatic properties of Grx1p have recently been characterized in detail using a fusion between a redox-sensitive version of yellow fluorescent protein (rxYFP) and yeast Grx1p, where the redox potential of the glutathione thiol–disulfide equilibrium can be directly monitored through changes in the fluorescence of the YFP moiety. These studies suggested that the glutathionylated intermediate of Grx1p may be highly stabilized in favour of the disulfide form, even though Grx1p is a dithiol enzyme. In order to understand the underlying molecular nature of this stabilization, we were interested in obtaining structural information on the glutathionylated intermediate. This intermediate can be produced quantitatively by glutathionylation of the mutated version of Grx1p containing only a single cysteine residue (C30S).

Here, we report the three-dimensional structure of glutathionylated yeast C30S Grx1p, the first published structure of a eukaryotic glutaredoxin. A mutant form of the enzyme was used in which the second active-site cysteine was mutated to a serine residue. This mutant form was then glutathionylated on the remaining cysteine residue (Cys27). The structure of a fusion protein consisting of yellow fluorescent protein, a linker region and reduced Grx1p C30S is also described. We used a rather unconventional approach to solve the Grx1p structure by first solving the structure of the fusion protein by molecular replacement with the rxYFP moiety as a search model and then building the Grx1p domain. This made heavy-metal screening and tedious molecular-replacement attempts with distantly related structures superfluous.

2. Methods

The two proteins, yeast glutaredoxin Grx1p C30S mutant and the fusion protein consisting of redox-sensitive yellow fluorescent protein (rxYFP) N-terminally linked to Grx1p C30S, were purified, crystallized and flash-frozen as described previously (Bjornberg *et al.*, 2006; Håkansson *et al.*, 2006). Synchrotron data were collected at beamline 7-11 at MAX-lab, Lund, Sweden. The data were reduced using *MOSFLM* and the *CCP*4 program suite (Collaborative Computational Project, Number 4, 1994; Leslie, 1992; Table 1). The structure of the fusion protein was solved by molecular replacement using the *CCP*4 version of *AMoRe* and the structure of redox-

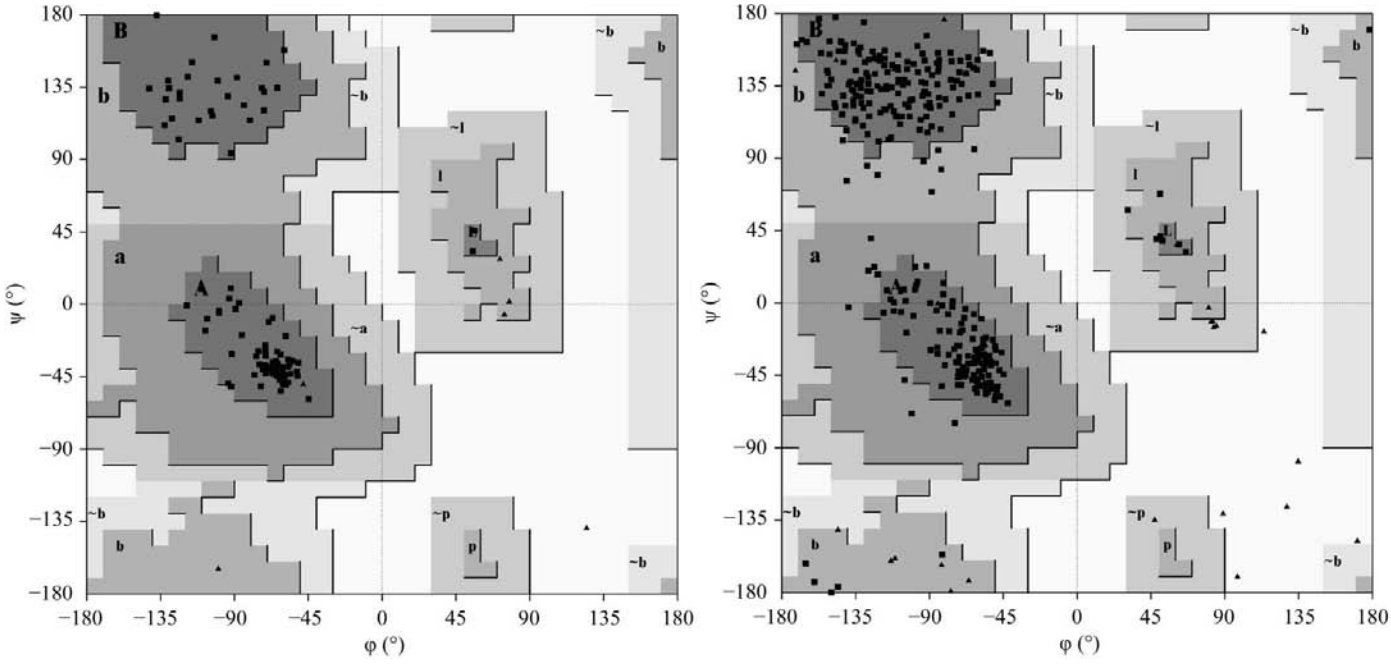

Figure 1
Ramachandran plots of (*a*) the orthorhombic glutathionylated Grx1pC30S crystal structure and (*b*) the hexagonal rxYFP-Grx1p C30S fusion protein crystal structure.

Table 1
Refinement statistics.

Data statistics have been published elsewhere (Håkansson *et al.*, 2006).

	Glutathionylated Grx1p C30S	rxYFP-C30S Grx1p fusion protein
Resolution range (Å)	20–2.02	20.2–2.7
R (%)	20.8	21.4
R_{free} (%)	24.3	25.7
R.m.s.d. bond lengths (Å)	0.0045	0.0061
R.m.s.d. angles (°)	1.23	1.36
R.m.s.d. dihedral angles (°)	22.4	25.0
R.m.s.d. improper angles (°)	0.69	0.80
Protein/glutathione atoms	875	2753
Water/sulfate atoms	66	65
B_{ave} (Å^2)	27.1	51.9
Luzzati coordinate error (Å)	0.23	0.33
Ramachandran most favoured/ additional allowed (%)	97.9/2.1	89.3/10.7

sensitive yellow fluorescent protein as the search model (Navaza, 1994; Ostergaard *et al.*, 2001). The phases obtained from this model (approximately two-thirds of the total structure) were sufficient to calculate electron-density maps from which the glutaredoxin moiety could be built. In the first maps, electron density for several glutaredoxin β-strands was clearly seen and the position of some of the conserved residues could be identified by looking at the Prx5 structure. The maps improved as more and more of the structure was defined and the phases were recalculated. Refinement and electron-density map calculations were performed with *CNS* and the results were visualized using the graphics program *O* (Brünger *et al.*, 1998; Jones *et al.*, 1991). Once this structure had been built and refined, its glutaredoxin part was used to solve the structure present in the orthorhombic glutaredoxin crystal. As the orthorhombic crystals diffracted to a better resolution (2.02 Å) and the refined structure was of a superior quality, it was used as a starting model for a second refinement of the glutaredoxin moiety in the rxYFP-Grx1p fusion protein (2.7 Å). The orthorhombic form was refined with individual B factors and the fusion protein with group B factors. In both cases, special care was taken to limit the overall number of refinement cycles in order to minimize the gap between R and R_{free} (Brünger, 1992). Hence, manipulations based on refined maps were often performed on the starting model (rather than on the refined structure), which was then refined *de novo*. Data statistics have been published elsewhere (Håkansson *et al.*, 2006) and refinement statistics are shown in Table 1. Ramachandran plots are shown in Fig. 1.

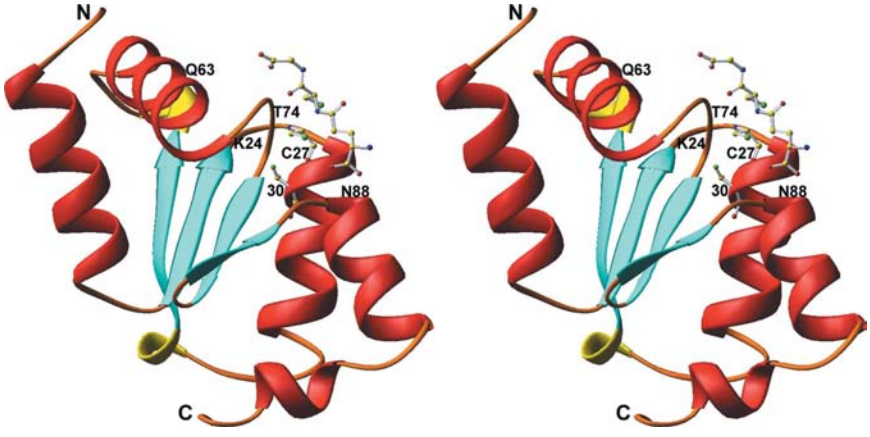

Figure 2
Stereo image showing the fold of yeast Grx1p glutaredoxin (Carson, 1991). The glutaredoxin fold has been coloured according to the secondary structure, with α-helices in red, 3_{10}-helices in yellow, β-strands in blue and the remainder of the protein in orange. The bound glutathione moiety and Cys27 along with the mutated Ser30 are shown in ball-and-stick representation. C, O, N and S atoms are coloured yellow, red, cyan and green, respectively. The oxygen of the mutated Ser30 has been coloured green as it represents the wild-type Cys residue. The positions of some other amino-acid residues interacting with glutathione are indicated, although the side chains have not been pictured.

3. Results and discussion

3.1. Overall fold and comparison with other glutaredoxins

The structure of glutathionylated glutaredoxin Grx1p C30S mutant was determined from Met1 to Leu108. The absence of electron density attributable to the last two residues (Ala109 and Asn110) precluded structural assignment of the C-terminus. The glutathione bound at the active site was clearly visible and could easily be defined. The fold of Grx1p, shown in Fig. 2, follows the same trace as that of previously determined glutaredoxin structures, with a central four-stranded mixed β-sheet with topology -1x, 2, 1 (Richardson, 1981). There are five helices: one at the N-terminus, one between strands 1 and 2, one between strands 2 and 3 and two at the C-terminus. The simple hairpin connection between strand 3 and 4 is the only part of the β-sheet where the strands are not interleaved with an α-helix. Superimposition of residues Met1–Leu108 of the orthorhombic crystal structure with the fusion protein rxYFP-Grx1p (free reduced C30S mutant) results in an r.m.s. deviation of only 0.5 Å, indicating that no conformational change takes place upon mono-oxidation of Grx1p. Naturally, the structures of the β-strands agree somewhat better than the helices. The maximum displacement is 1.3 Å and the differences in side-chain conformations are also modest. Thus, the presence of a glutathione molecule in the active site does not induce larger changes than those expected for the same protein in two different crystal environments. This is in agreement with the crystallographically elucidated structures of the related cDsbD, indicating a rigid domain that does not undergo any conformational changes upon oxidation/reduction (Stirnimann *et al.*, 2006). In contrast, the structures of the oxidized, reduced and mixed-disulfide forms of *E. coli* Grx1 were reported to differ as observed by NMR spectroscopy (Bushweller *et al.*, 1994; Sodano *et al.*, 1991; Xia *et al.*, 1992).

The structure was superimposed with the crystal structures of human Grx2 (PDB code 2fls) and the glutaredoxin domain of *H. influenza* Prx5 (PDB code 1nm3; Kim *et*

al., 2003), initially by minimizing the distance between selected active-site residues. The resulting structural alignment was used to identify identical and homologous amino acids in the proteins. Next, the homologous C^{α} positions of residues 6–39 and 50–107 in Grx1p were superimposed on the human Grx2 residues 16–49 and 56–102 with an r.m.s.d. of 1.2 Å. Omitting the N-terminal and the C-terminal helices in the procedure gave an r.m.s.d. of 0.7 Å for the remaining 80 residues. Superimposing the C^{α} positions of residues 19–39 and 63–94 with the homologous positions in *H. influenza* Prx 5 resulted in an r.m.s.d. of 1.1 Å. The most conspicuous difference between the structures is that Prx5 glutaredoxin domain, which is preceded by a peroxiredoxin domain, lacks the first and last helix found in yeast and human glutaredoxin. Moreover, the third helix, between β-strands 2 and 3, is shorter and has a more irregular structure in *H. influenza* Prx 5 compared

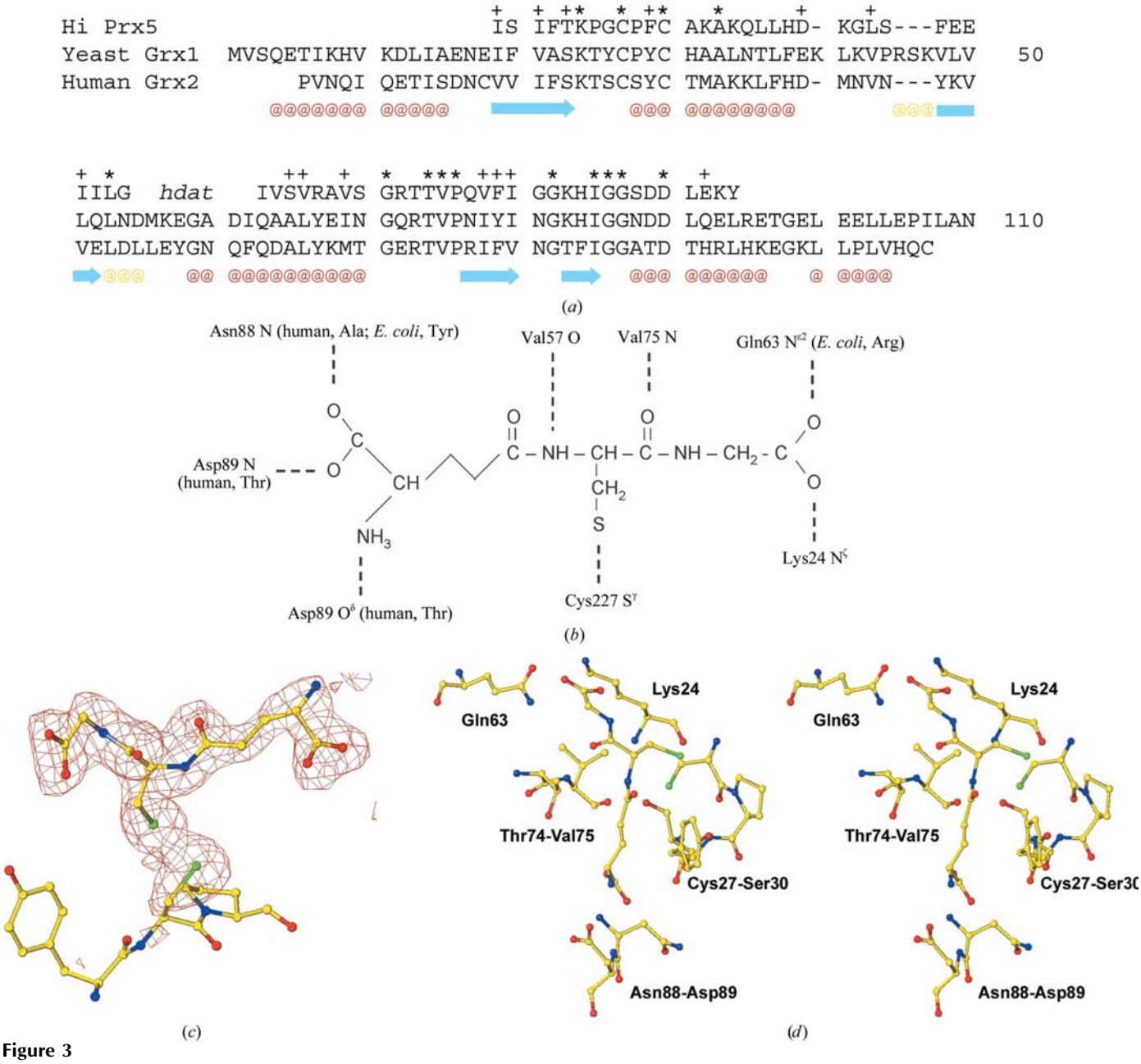

Figure 3

(*a*) Structure-based alignment of yeast Grx1p with its two most closely related sequences from crystallographic structures in the PDB: human Grx2 and *H. influenzae* Prx5 (Kim *et al.*, 2003). Consensus residues are marked with an asterisk (14 residues out of 110) and residues that were all homologues belonging to any of the groups (S, A, T), (D, E, N, Q, H), (F, Y) or (K, R) are marked with a '+' (14 residues out of 110). Residues without any homologues are in italics. The secondary-structure elements in yeast Grx1p are shown below the sequences, with β-strands shown as blue arrows and α-helices and 3_{10}-helices indicated by '@' in red and yellow, respectively. (*b*) Schematic representation of the glutathione–glutaredoxin interactions. Where the homologous residues in human Grx2 or *E. coli* Grx3 differ from the amino acids in Grx1p, this is indicated in parentheses. (*c*) $|F_o| - |F_c|$ electron-density maps calculated after refining a model lacking the glutathione ligand and the Cys27 side chain superimposed on the final coordinates for these atoms. (*d*) Ball-and-stick representation of glutathione and the active site of Grx1p C30S, illustrating the position of glutathione sandwhiched between Thr74 and Tyr29. The view is 'from the right' in Fig. 2.

with the other two glutaredoxins. The absence of the terminal helices is a feature Prx5 shares with the more distantly related T4 glutaredoxin (Eklund *et al.*, 1992), although this protein has a longer helix between strands 2 and 3. Otherwise, the backbones of the four proteins are most similar from the T_{74}VP motif and onward, *i.e.* the second folding unit consisting of β-strands 3 and 4 (Eklund *et al.*, 1992). Sequence alignments based on the structural superimpositions of yeast Grx1p, human Grx2 and *H. influenza* Prx5 are shown in Fig. 3(*a*).

3.2. Glutathione-binding site

The binding of glutathione in the active site of Grx1p C30S was evident from crystal analysis of the derivative. The two O atoms of the α-carboxylate group of the glutathione glutamate are hydrogen bonded to the main-chain amino groups of Asn88 and Asp89, respectively. These two residues are situated at the N-terminus of helix Asn88–Glu96, with the protein–ligand interaction backed up by the dipole moment of the helix. The N-terminal amino group of glutathione is hydrogen bonded to the side chain of Asp89. The main-chain amino and carbonyl groups of the glutathione cysteine residue are hydrogen bonded to the backbone of Val75, which together with the preceding Arg73 and Thr74 forms a segment in β-strand conformation perpendicular to the subsequent Asn77–Ile80 β-strand. Pro76, with a *cis*-isomer amide bond, links this short β-segment to the subsequent β-strand. The C-terminal carboxylate O atoms of the glutathione glycine residue are hydrogen bonded to the side chains of Lys24 and Asn63. The mutated C30S and the glutathione S atom are on opposite sides of the Cys27 S atom, in agreement with these two groups substituting each other in the putative reaction cycle of the enzyme. A schematic representation of the ligand–protein interactions is shown in Fig. 3(*b*).

An unexpected feature of the glutathione binding was that the covalent bond between the glutathione cysteine and Cys27 was broken. Initial leashing of these two groups with a covalent S—S bond resulted in poorly fitted electron-density maps with negative $F_o - F_c$ density between the two S atoms and positive $F_o - F_c$ density on either of the opposite sides. Refinement of the structure after deletion of first one of the two S^{γ} atoms and then of the other led to S^{γ}-atom positions that were 2.7 Å apart. As this is much longer than a covalent bond (2.0 Å), it was regarded as a hydrogen bond and the final restrained refinement with all atoms present resulted in an S—S distance of 2.9 Å. The lability of redox-active intracellular cysteine residues was recently observed in the structure of yeast protein disulfide isomerase (Tian *et al.*, 2006) and in the radiation-induced cleavage of the disulfide bond in oxidized cDsbD (Stirnimann *et al.*, 2006). The two active-site cysteines in protein disulfide isomerase were best modelled as a mixture of reduced and oxidized forms with partial occupancy. In the case of cDsbD, the progress of reduction could be followed by processing and comparing partial data sets (collected to 1.1 Å) from the beginning and the end of data collection, observing S—S distances from 2.4 to 3.0 Å. In contrast, a completely chemically reduced specimen showed a distance of 3.5 Å between the two cysteines. It was concluded that photoreduction was never complete. In the case of yeast Grx1p, there was no indication of crystal disorder or mixed occupancy. An alternative explanation is that photoreduction is complete but that the diffusion of the glutathione from the observed position to a longer and more favourable distance is more or less halted at 100 K. For the same reason, we believe that the conformation of the protein is representative of the mono-oxidized state, leading to the conclusion that mono-oxidation does not induce any conformational changes (§3.1). A similar distance between the two S atoms is found in the recently deposited, but unpublished, human Grx2 structure. The difference Fourier map around the final glutathione-binding site is shown in Fig. 3(*c*).

The side chain of residue Ser30, which in the wild-type enzyme is the second active cysteine residue, is well positioned for nucleophilic attack on the Cys27 S atom. This result differs from the NMR analysis of the similarly glutathionylated Cys to Ser mutant of *E. coli* Grx3 (Nordstrand *et al.*, 1999), where the hydroxyl group of the serine residue was turned the opposite way and thus not ready for bond formation. The χ_1 values in the two structures differ by about 160°. Overall, the glutathione-binding position is similar in the yeast Grx1p crystallographic structure and the NMR study of *E. coli* Grx3, but there are some differences. In the *E. coli* Grx3 the glutathione cysteine is closer to the protein, since the covalent link to the active-site cysteine is intact. The N-terminal glutathione Glu residue on the other hand is closer to the protein

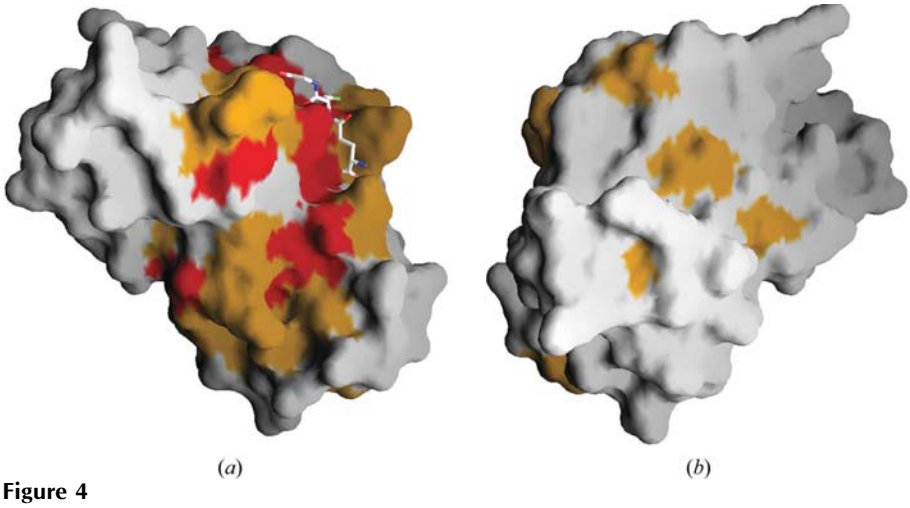

Figure 4
Conserved residues mapped on the surface of Grx1p. Residues that are absolutely conserved in Grx1p, human Grx2 and *H. influenzae* Prx5 are mapped in red and residues that are conserved in Grx1p and one of the other two sequences are mapped in orange. (*a*) A view from approximately from the same direction as in Fig. 2. (*b*) The molecule is rotated in order to show the opposite side.

body in the crystallographic structure, where Pro28, Tyr29 and the N-terminal α-carboxylate group of glutathione are stacked at distances of 4.5 Å. In the NMR study, the homologous Tyr residue has a different conformation and the N-terminus of glutathione has a different position and orientation around the Glu $C^{\alpha}-C^{\beta}$ bond, leading to different orientations of the carboxylate group and the amino group. The orientation of the C-terminal carboxylate of the glutathione Gly residue is directed towards the enzyme in the crystallographic structure and away from the enzyme in the NMR study. The opposite is true for the amino group, which in the NMR study hydrogen bonds to the side chain of Thr74 (Grx1p numbering). The role of Tyr29 and the position of the glutathione ligand in the cleft between Tyr29 and Thr74 are shown in Fig. 3(*d*).

3.3. Conserved residues

The structure-based alignment shown in Fig. 3(*a*) of the Prx5 glutaredoxin domain, human Grx2 and yeast Grx1p results in 14 residues that are conserved among the three enzymes. Some of these have obvious catalytic or substrate-binding roles. Lys24 hydrogen bonds to the glutathione C-terminal carboxylate group and Cys27 and Cys30 are redox-active, while the role of Ala33, on the distal side of Cys30, is more obscure. The T_{74}VP motif aligns the glutathione moiety. The lack of side chains on the two glycines in the I_{85}GG motif prevents steric interference with Asp90 and the glutathione substrate, respectively, while the isoleucine firmly anchors this stretch in a hydrophobic cluster. Interactions between this conserved motif and the conserved Asp90 further stabilize the strand–helix connection between them. This connection interacts with the glutathione glutamate α-carboxylate group through the backbone amino groups of residues Asn88 and Asp89. It is noteworthy that Asp89 is not conserved; the hydrogen bond between Asp89 and the N-terminal amino group of glutathione is replaced by a hydrogen bond between a threonine and the glutathione glutamate α-carboxylate group in the crystal structure of human Grx2, as well as in the NMR structure of *E. coli* Grx1 (Bushweller *et al.*, 1994). Four of the residues that are conserved in the three enzymes yeast Grx1p, human Grx2 and *H. influenza* Prx5 are situated far from the active site and are probably not essential for glutathione binding.

Fig. 4 shows a surface representation of yeast Grx1 with residues conserved in yeast Grx1, human Grx2 and *H. influenza* Prx5 shown in colour. It can be seen that in addition to the active-site pocket, there is a relatively broad band of conserved/semiconserved residues on the surface of the protein from the glutathione-binding site along the 'second folding motif', which is also the region where the structures superimpose best. There are relatively few conserved residues on the opposite side of the molecule.

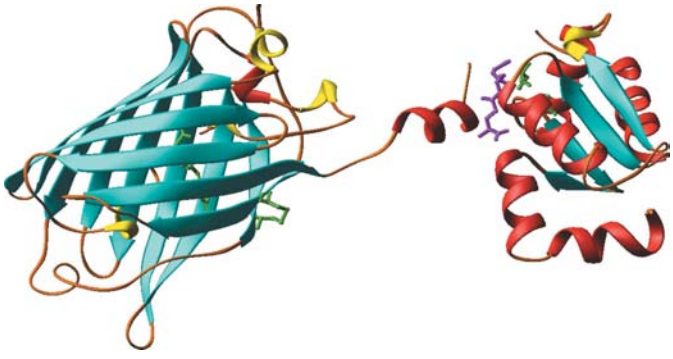

Figure 5
RIBBONS representation (Carson, 1991) of the rxYFP-Grx1p fusion protein. The chromophore and the disulfide bridge of the rxYFP moiety and the two active-site cysteines of Grx1p (one of which is mutated in the crystal structure) are shown in green ball-and-stick representation and the supposed position of the glutathione is shown in magenta. The glutathione position was obtained by superimposing the Grx1p C30S–glutathione structure on the Grx1p domain of the fusion protein.

3.4. Structure of the rxYFP-C30S glutathione fusion protein

Fig. 5 shows the structure of the rxYFP-Grx1p C30S fusion protein together with the glutathione position obtained by superimposition of the Grx1p C30S–glutathione structure. The electron density of the linker region was weak and residues Gly242–Ser245 were not defined. Residues Tyr237–Ser241 had ill-defined side chains and were built as Ala-Ala-Ala-Gly-Gly. The closest distance between Ser241 and Gly246 of any symmetry-related glutaredoxin domain exceeds 40 Å, which cannot be covered by only four missing residues. The glutaredoxin domain in the crystal structure is therefore unambiguously matched with the correct rxYFP domain, despite the gap in the linker region.

There are no contacts between the two domains of the fusion protein in the crystal structure. While domain structures are stable and usually unaffected by crystallization, domain–domain orientations may be influenced by crystal packing if the energy difference between different conformations is small. As judged by the partly extended and apparently flexible linker region, this is probably the case for the rxYFP-Grx1p fusion protein. In the conformation found in our crystallographic analysis, the rxYFP disulfide bridge is actually turned towards the glutaredoxin domain, but not towards any conserved region or the active site. The linker region partly covers the glutathione-binding site, with the potential for both constructive interactions (His234 carbonyl group and the N-terminal amino group of glutathione) and nonconstructive steric interference between protein and glutathione. It is most likely that the two domains of the fusion protein are tethered only by the linker region in solution and with only temporary domain–domain interactions. The enhanced exchange of reducing equivalents in solution between the two domains (Bjornberg *et al.*, 2006) is probably a consequence of the limited distance and enhanced collision rate between the two components rather than any specific interaction.

4. Conclusion

We have determined the three-dimensional structure of yeast Grx1p in complex with glutathione. The structure will be helpful for future studies of the redox potential and kinetics of

glutaredoxin glutathionylation. It will also be an invaluable guide for site-directed mutagenesis experiments aimed at characterizing glutathione–glutaredoxin interactions. The structure of the rxYFP-Grx1p fusion protein suggests that no high-affinity specific interactions between the redox sensor and Grx1p are necessary for this elegant construct to monitor redox changes and the status of glutathione in its environment.

We are grateful to professor Sine Larsen for sharing synchrotron beam time. The synchrotron data were collected at MAX-lab beamline 7-11 under the supervision of Dr Yngve Cerenius. This work was supported by the Danish Research Council.

References

Bacik, J. P., Brigley, A. M., Channon, L. D., Audette, G. F. & Hazes, B. (2005). *Acta Cryst.* F**61**, 550–552.

Berman, H. M., Westbrook, J., Feng, Z., Gilliland, G., Bhat, T. N., Weissig, H., Shindyalov, I. N. & Bourne, P. E. (2000). *Nucleic Acids Res.* **28**, 235–242.

Bjornberg, O., Ostergaard, H. & Winther, J. R. (2006). *Biochemistry*, **45**, 2362–2371.

Brünger, A. T. (1992). *Nature (London)*, **355**, 472–474.

Brünger, A. T., Adams, P. D., Clore, G. M., DeLano, W. L., Gros, P., Grosse-Kunstleve, R. W., Jiang, J.-S., Kuszewski, J., Nilges, M., Pannu, N. S., Read, R. J., Rice, L. M., Simonson, T. & Warren, G. L. (1998). *Acta Cryst.* D**54**, 905–921.

Bushweller, J. H., Billeter, M., Holmgren, A. & Wuthrich, K. (1994). *J. Mol. Biol.* **235**, 1585–1597.

Carson, M. (1991). *J. Appl. Cryst.* **24**, 958–961.

Collaborative Computational Project, Number 4 (1994). *Acta Cryst.* D**50**, 760–763.

Discola, K. F., Oliveira, M. A., Silva, G. M., Barcena, J. A., Porras, P., Padilla, A., Netto, L. E. & Guimaraes, B. G. (2005). *Acta Cryst.* F**61**, 445–447.

Eklund, H., Ingelman, M., Soderberg, B. O., Uhlin, T., Nordlund, P., Nikkola, M., Sonnerstam, U., Joelson, T. & Petratos, K. (1992). *J. Mol. Biol.* **228**, 596–618.

Fernandes, A. P. & Holmgren, A. (2004). *Antioxid. Redox Signal.* **6**, 63–74.

Håkansson, K. O., Østergaard, H. & Winther, J. R. (2006). *Acta Cryst.* F**62**, 920–922.

Jones, T. A., Zou, J.-Y., Cowan, S. W. & Kjeldgaard, M. (1991). *Acta Cryst.* A**47**, 110–119.

Kim, S. J., Woo, J. R., Hwang, Y. S., Jeong, D. G., Shin, D. H., Kim, K. & Ryu, S. E. (2003). *J. Biol. Chem.* **278**, 10790–10798.

Leslie, A. G. W. (1992). *Jnt CCP4–ESF/EACMB Newsl. Protein Crystallogr.* **26**.

Navaza, J. (1994). *Acta Cryst.* A**50**, 157–163.

Nordstrand, K., Aslund, F., Holmgren, A., Otting, G. & Berndt, K. D. (1999). *J. Mol. Biol.* **286**, 541–552.

Ostergaard, H., Henriksen, A., Hansen, F. G. & Winther, J. R. (2001). *EMBO J.* **20**, 5853–5862.

Richardson, J. S. (1981). *Adv. Protein Chem.* **34**, 167–339.

Sodano, P., Xia, T. H., Bushweller, J. H., Bjornberg, O., Holmgren, A., Billeter, M. & Wuthrich, K. (1991). *J. Mol. Biol.* **221**, 1311–1324.

Stirnimann, C. U., Rozhkova, A., Grauschopf, U., Bockmann, R. A., Glockshuber, R., Capitani, G. & Grutter, M. G. (2006). *J. Mol. Biol.* **358**, 829–845.

Tian, G., Xiang, S., Noiva, R., Lennarz, W. J. & Schindelin, H. (2006). *Cell*, **124**, 61–73.

Xia, T. H., Bushweller, J. H., Sodano, P., Billeter, M., Bjornberg, O., Holmgren, A. & Wuthrich, K. (1992). *Protein Sci.* **1**, 310–321.